05 Apr 1995, 1:30 pm - 3:30 pm

Improved Soil-Spring Method for Soil-Structure Interaction — Vertical Excitation

A. H. Hadjian
Defense Nuclear Facilities Safety Board, Washington, D.C

H. T. Tang
EPRI, Palo Alto, California

Proceedings: Third International Conference on Recent Advances in Geotechnical Earthquake Engineering and Soil Dynamics, April 2-7, 1995, Volume I, St. Louis, Missouri

Improved Soil-Spring Method for Soil-Structure Interaction - Vertical Excitation

Paper No. 5.14

A.H. Hadjian
Sr. Technical Staff, Defense Nuclear Facilities Safety Board, Washington, D.C.

H.T. Tang
Project Manager, EPRI, Palo Alto, California

SYNOPSIS An improved Soil-Spring Method for vertical response analysis is proposed. The Soil-Spring Method belongs to the substructuring methods of analyses for seismic soil-structure interaction. As originally developed the method has certain significant limitations. The proposed improvement is essentially iterative where, successively, layering, embedment, soil damping and frequency-dependent effects are introduced and adjusted until acceptable convergence is achieved. Additionally, input motion for embedded structures is specified using a simple procedure. The metholodogy is applied to the Lotung 1/4-scale containment model for three recorded earthquakes. The comparisons of the response results with the recorded data and with results obtained using state-of-the-art methods definitely establishes the improved Soil-Spring Method for seismic soil-structure interaction as an analysis tool at least comparable to the more sophisticated methods.

INTRODUCTION

The analysis for Soil-Structure Interaction (SSI) has progressed from simple Winkler type models to sophisticated methods such as CLASSI (Luco et al, 1979) and SASSI (Lysmer et al, 1981). An evaluation of SSI methodologies practiced in the US (Hadjian et al, 1991), clearly indicates that, given correctly specified soil-structure models, adequate response results can be obtained by both SASSI and CLASSI. It was also concluded that more than the computational methods, the adequacy of the response results are due to the modeling of the soil-structure system and the characterization of the input motions. Therefore, it is to be expected that simpler methods, such as the soil spring method (Richart et al, 1970), could be modified to produce results similar to SASSI and CLASSI based on a clearer understanding of the basic elements of SSI.

Enhancing the basic soil-spring model can proceed in two distinct paths: a) an additional set of masses, springs, and dashpots is added to the basic soil-spring representation of the supporting medium to directly account for frequency dependency and embedment effects, and b) an iterative approach that corrects for frequency dependency and embedment effects at each cycle. The latter is the method of choice in this paper.

The prime objective of this investigation is to develop a cost-effective viable methodology. This paper deals with the vertical excitation case only. An earlier paper presented the case for horizontal excitation (Hadjian and Tang, 1992). The complete study, including both horizontal and vertical excitations is reported in an EPRI report (Hadjian, 1991 and 1993).

Considering page limitations, it would be impossible to describe all of the details of the improved Soil-Spring Method. Thus, the following is a summary extraction of the steps of the analysis used and some selected results from the subject EPRI Draft Final Report (Hadjian, 1993).

THE IMPROVED SOIL-SPRING METHOD

The Soil-Spring Method (SSM) belongs to the substructuring methods of analyses for seismic SSI. As originally developed (Richart et al, 1970), the SSM has the following significant limitations:

Requires a uniform half-space characterization of the foundation
Spring and dashpot parameters are frequency-independent
Embedment effects are not directly included
Soil material (hysteretic) damping is ignored
Input motion is simply the free-field ground surface motion

The analysis by the proposed improved SSM is iterative where, successively, layering, embedment, damping and frequency-dependent effects are introduced and adjusted until acceptable convergence is achieved. For this study, all the possible adjustments are incorporated whether their impact is large or small.

Besides its relative simplicity and being highly noncomputer-intensive, the main attractions of the iterative SSM are the freedom it provides to make decisions at each step of the solution path to reflect experience and real world physical realities that would be very difficult to model otherwise, and the opportunity it provides to investigate frequencies, mode shapes and modal damping values before a final response calculation is performed. These investigations of the eigenparameters provide insight into the nature of the response. As an example, for the Lotung 1/4-scale model, the mode shapes and associated damping values clearly indicate the irrelevance of the first, primarily the rocking mode, to the horizontal response of the structure at its base. The base horizontal response is due primarily to the highly damped second translation-rocking mode. Therefore, as expected, the response predictions at the base have been more successful than response predictions at the top of the structure (Hadjian et al, 1991), since the latter depends on the adequate prediction of the system fundamental frequency.

The methodology is applied to the Lotung 1/4-scale containment model (Tang, 1987) for three events: LSST06, LSST07 and LSST16. Characteristics of these events are listed in Table 1.

ANALYSIS STEPS

The following steps are required to perform a good SSI analysis by the improved SSM.

Table 1. Characteristics of Three Seismic Events Used in Study

Event	Date	Magnitude	Epicentral Distance (km)	Focal Depth (km)	Peak Acceleration (g)
LSST06	04-08-86	5.4	31	11	0.04
LSST07	05-20-86	6.5	66	16	0.21
LSST16	11-14-86	7.0	78	7	0.17

Step 1. Modeling of the Fixed Base Structure

A lumped-mass model, if properly constructed, is deemed appropriate. Obviously the method allows for the use of detailed finite element models so long as the structure and foundation impedances are brought together at an interface node. The lumped-mass model is used in this study.

Figure 1 shows a cross section of the 1/4-scale containment model constructed at Lotung. For details of this model the reader is referred to Tang (1987) and Hadjian et al (1991). The fundamental vertical mode frequency is 34.63 Hz. For seismic excitations the structure may therefore be considered rigid.

Step 2. Site Characterization

There are two substeps in characterizing the site before the soil-spring and dashpot parameters could be calculated.

2.1 Low-Strain Characterization

Following geophysical site investigations and laboratory tests (these are generally common to all methods of analysis) the site is characterized as a horizontally layered medium with the following low amplitude ($\sim 10^{-4}$% shear strain) properties for each layer:

- G - shear modulus
- E - elastic modulus
- ν - Poisson's ratio
- ρ - mass unit weight
- V_s - shear wave velocity
- V_p - compressional wave velocity
- β_s - material soil damping for V_s
- β_p - material soil damping for V_p

Embedment backfill properties are also critical for an adequate SSI analysis. Similar properties as those for the free-field must be developed. However, for the Lotung project, the backfill properties in this analysis are assumed to be the same as the free-field data, based on the Ohsaki Research Institute (1989) geophysical test report on the backfill.

The solid lines in Fig. 2 are an idealized representation of the site low-strain wave velocities based on the geophysical test data by Anderson (1991). Also shown in Fig. 2 are the layers into which the soil profile is subdivided for computational purposes. The layer properties shown on the right hand side of the figure are simply average layer values. Poisson's ratio, ν_L, for each layer is calculated from the following relationship:

$$\frac{V_s}{V_p} = \sqrt{\frac{1-2\nu}{2(1-\nu)}} \tag{1}$$

Equations 2 and 3 can then be used to calculate G and E given ρ:

$$G = \rho V_s^2 \tag{2}$$

and

$$E = 2G\,(1+\nu) \tag{3}$$

Thus, the free-field is completely characterized for low-strain SSI analysis.

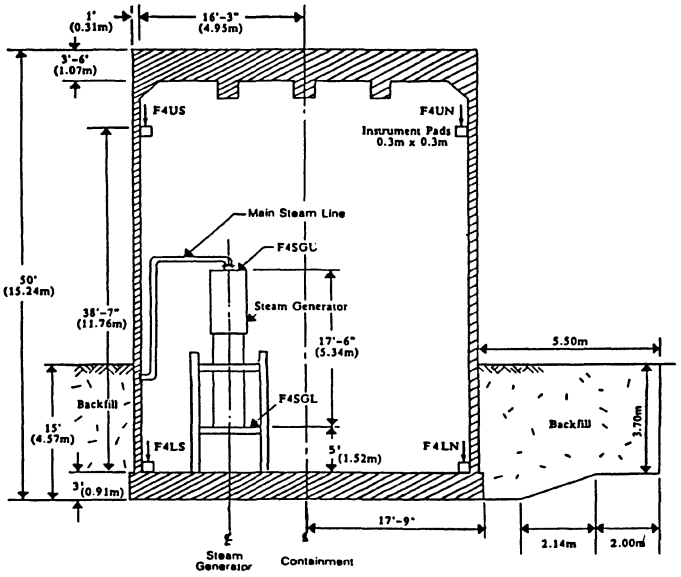

Fig. 1. Cross-Section of the 1/4-Scale Containment Model

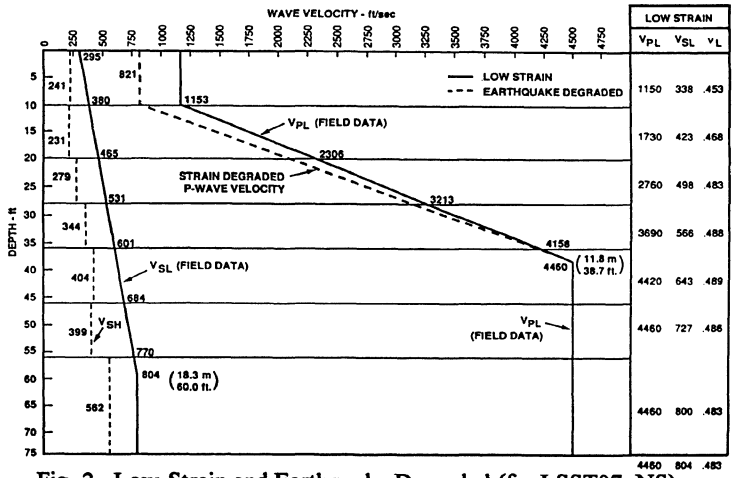

Fig. 2. Low-Strain and Earthquake Degraded (for LSST07, NS) S- and P-wave Profiles and Low-Strain Poisson's Ratios, ν_L

2.2 Strain-Degraded Soil Properties

Based on a site appropriate shear modulus stiffness degradation curve, earthquake specific site and backfill soil profiles are generated by use of the SHAKE computer code (Schnabel et al, 1972). Invariably the EW, NS and vertical profiles tend to be different depending on the level of shaking in each respective direction. These differences are maintained in subsequent response calculations.

In order to avoid uncertainties in developing the strain degraded soil profiles (stiffness and damping), it was decided to use the profiles obtained by Geomatrix Consultants (1991). These profiles were obtained using the site-specific shear stiffness degradation curves derived from actual earthquake response data at Lotung. All the free-field site response analyses are based on the motions recorded at station FA1-5 [see Tang (1987) for details of the site instrumentation], assumed to be representative of the free-field motions at the containment.

To complete the site characterization for each event and each component the P-wave related damping values are calculated from Eq. 4 (Luco and Wong, 1989),

$$\beta_p = \frac{4}{3}\left[\frac{V_s}{V_p}\right]^2 \beta_s \qquad (4)$$

where β_s, is the soil damping values from the SHAKE analysis.

Step 3. Equivalent Half-Space

Since the impedance coefficients for the SSM are based on the uniform half-space, an equivalent half-space model must first be developed based on the layered site characterization of the previous step and the foundation model. As shown in Fig. 3, two uniform properties of the site are needed: one for below the basemat and one for the embedment depth. Developing the properties for the embedment depth is relatively straightforward: it is a simple average of the layer moduli from the surface to the base level of the structure. The derivation of the uniform properties for the below-foundation medium is described below.

3.1 Structure Weight Effect on V_s

Given the strain-degraded free-field site characterization data, the moduli of the soil medium below and in the immediate vicinity of the foundation must be modified to account for the stiffening effects of the dead load of the superstructure (Prange, 1965).

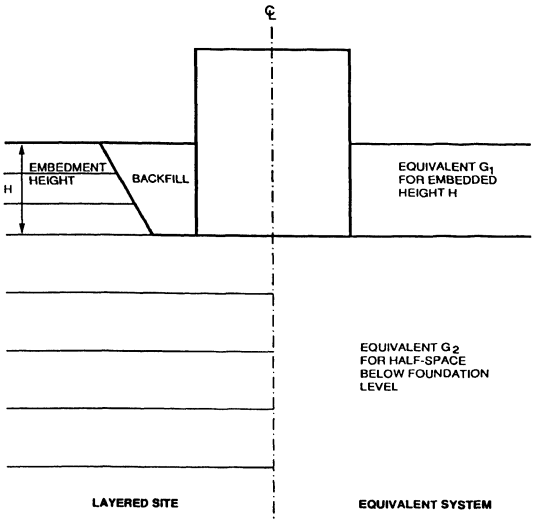

Fig. 3. Equivalent Parameters for Embedded Structures

For the Lotung 1/4-scale containment the average pressure due to the weight of the structure and the effect of the excavated soil just about balance each other out. Thus, there is no reason to carry out an adjustment of the wave velocity profiles.

3.2 Equivalent Half-Space for Impedances

Any procedure to estimate an equivalent half-space must consider the extent of the influence of the foundation on each of the affected layers. Hadjian and Ellison (1985) present such a procedure based on the static loading of the medium. Since the influence of each degree of freedom loading would reach a different depth, each degree of freedom of response would therefore result in its own unique half-space equivalent properties. Differences in moduli exist among the earthquakes, the directions of excitation and the degrees of freedom.

3.3 Equivalent Soil Material Damping

A SHAKE analysis provides soil material damping values for each of the layers used in the analysis. Similar to the determination of an equivalent soil shear modulus discussed above, the layer damping values must be similarly averaged for use in the SSM. The same procedure used for the calculation of the equivalent shear modulus is also used to calculate the soil damping values. These values are then multiplied by a factor of 0.75 to account for layering effects (Hadjian and Ellison, 1985).

Step 4. Impedances

The calculation of impedances follows the generally used expressions by Richart et al (1970) for surface foundations. For the vertical response the equivalent spring constant and damping coefficient are respectively given by

$$k_z = \frac{4GR}{1-\nu} \quad \text{and} \quad c_z = 0.85\, k_z R\sqrt{\frac{\rho}{G}} \qquad (5)$$

The impedances are subsequently modified for frequency dependency and embedment effects.

4.1 Surface Foundations

One of the improvements being introduced herein is the adjustment of the impedances for frequency dependency. Figure 4 shows the ratios by which Eq. 5 impedances need to be modified for the subsequent run as a function of the last cycle dimensionless frequency, a_0 (see Step 4.3). The curves are based on an earlier work by Luco (1976). The choice of material damping for c_{vv} in Fig. 4 is based on the fact that for the presently recommended procedure, the soil material damping is calculated from a separate SHAKE analysis and added to the radiation damping effects.

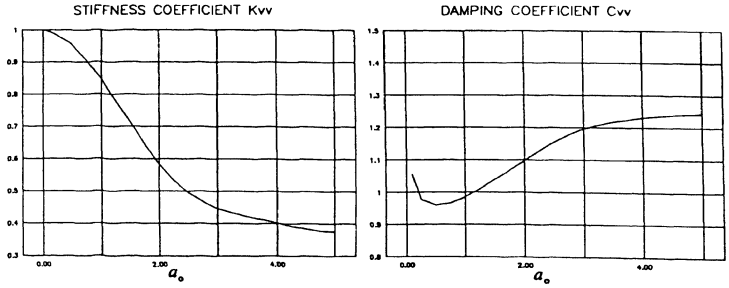

N.B. The stiffness factors are based on viscoelastic half-space with ξ = 0.05 and the damping factors with ξ = 0.005.

Fig. 4. Modification Factors for Frequency Dependency of Impedances (from Luco, 1976)

4.2 Embedded Foundations

Impedances for surface foundations can be modified to account for embedment effects. The modifications used are from Bechtel Topical BCTOP4 (Revised 1992) and are given by the following expressions:

$$k'_{ii} = k_{ii}\left[1 + (a_{ii} - 1)\frac{G_1 f_1}{G_2} f\right] \quad (6)$$

and

$$c'_{ii} = c_{ii}\left[1 + (\beta_{ii} - 1)\sqrt{\frac{G_1 f_1}{G_2}} f\right] \quad (7)$$

where

k_{ii} and c_{ii} are the frequency dependent surface impedances (from Step 4.1 above), and α_{ii} and β_{ii} are ratios of embedded to surface foundation impedances based on a uniform half-space. Charts giving these ratios as a function of the embedment ratio, H/R, and the dimensionless frequency, a_0 have been developed based on data from Aspel (1979). It is noted that relative to the embedment ratio the effect of a_0 in general is not that significant;

G_1 is the equivalent shear modulus of the embedment depth layer;

f_1 is a factor that recognizes the variation of G_1 with depth in real soils. Assuming that G_1 is simply the average of the variable G for the depth H, it can be shown that f_1 has a value of 1.0 for translational and 0.7 for rocking motions;

G_2 is the equivalent shear modulus of the half-space below the foundation (Fig. 3);

f is an empirically derived factor to account for soil-structure interface conditions different from the theoretical welded condition on which α_{ii} and β_{ii} are based. It depends primarily on the level of shaking, the amount of perimetral embedment and the degree of the backfill compaction.

4.3 System Dimensionless Frequency

In order to successively improve the values of the problem parameters, the system dimensionless frequency must be calculated at the end of each cycle. The system dimensionless frequency is given by

$$a_o = \frac{\omega_d R}{V_{se}} \quad (8)$$

where ω_d = the system damped frequency of interest
R = radius of foundation
V_{se} = equivalent shear wave velocity of system half-space

$$= \sqrt{\frac{G_e}{\rho}}$$

The system damped frequency is given by

$$\omega_d = \omega\sqrt{1 - \bar{\xi}^2} \quad (9)$$

where $\bar{\xi}$ is the system damping value. The use of ω_d is motivated by the facts that structures would respond to earthquakes at the damped system frequencies and that damping during SSI could be significant. G_e is a weighted average of G_1 and G_2 according to their contribution to the impedances for each degree of freedom and of the relative contributions of the translational-rocking modes to the system frequency.

Step 5. System Frequencies and Damping Values

This step primarily deals with the free-vibration problem and the generation of system damping values that also include the soil hysteretic damping effects. The process of calculating the system frequencies and damping values is iterative and the process is terminated when the dimensionless frequency, as described in Step 4.3 above, does not materially change from a previous cycle. This iterative approach seems to be robust, i.e., only three models are used to terminate the process:

1st Model - Surface structure and frequency independent impedances.

2nd Model - Frequency dependent and embedment effects incorporated with soil-springs and dashpots attached to base of model.

3rd Model - Incorporation of coupling terms by relocating the attachment of the soil-springs and dashpots to the center of resistance and a second modification for frequency dependency based on the revised system frequency.

5.1 First Model

Starting with the frequency independent impedances of the surface foundation (Eq. 5) and the equivalent half-space as characterized by G_2 and related parameters, the system frequencies and associated radiation damping values are calculated (Bechtel DYNAM program was used for both). The First Model analysis is completed by calculating the system equivalent shear wave velocity and system demensionless frequency according to the procedure presented in Step 4.3. These results are tabulated in Table 2.

5.2 Second Model

In the Second Model two improvements are introduced: the surface impedances are modified to reflect frequency dependent values and embedment effects are incorporated. Using appropriate charts described above and the dimensionless frequencies from the First Model (all assumed to be 1.42), the modification factors for frequency dependency and embedment are obtained.

Based on the above modification factors, the impedances for the Second Model are calculated. In Eqs. 6 and 7 the f factor is assumed unity. And finally, the Second Model analysis is completed by calculating the system equivalent shear wave velocity and system dimensionless frequency according to the procedure presented in Step 4.3. These results are tabulated in Table 2.

5.3 Third Model

For the Third Model, the data of the Second Model are modified due to the revised dimensionless frequencies calculated at the end of the Second Model calculations. The frequencies and radiation damping values are then calculated and, together with the soil material damping values (unchanged), are listed in Table 3, where f is system frequency; m, percent modal mass; β_r, percent radiation damping; and β_s, percent soil damping.

And finally, the Third Model analysis is completed by calculating the system equivalent shear wave velocity and system dimensionless frequency according to the procedure presented in Step 4.3. The results are tabulated in Table 2. The decision to terminate the iterations is based on the Third Model results for the horizontal excitation (see Hadjian and Tang, 1992). It will be noted in this reference that the change of the system dimensionless frequency of the Third Model from the Second Model is minor (1 to 2%) and hence the iterative process for successive improvements is terminated. Therefore, the frequencies and system damping values of Table 3 are used in the time-history response calculations to predict the recorded response of the 1/4-scale containment to three earthquakes.

Table 2. System Shear Wave Velocities (fps) and Dimensionless Frequencies

	First Model		Second Model			Third Model*		
	V_c	a.	V_c	a.		V_c	a.	
				Undamped	Damped		Undamped	Damped
LSST06-E	498	1.41	467	1.73	0.54	472	1.66	1.13
LSST06-N	514	1.42	481	1.72	0.58	472	1.66	1.13
LSST07-E	306	1.42	291	1.81	0.00	293	1.70	1.03
LSST07-N	316	1.42	297	1.77	0.24	293	1.70	1.03
LSST16-E	352	1.42	331	1.78	0.25	314	1.69	1.05
LSST16-N	316	1.42	298	1.79	0.00	314	1.69	1.05

*For this final calculation, a combined vertical model is used based on the average EW and NS site characteristics.

Table 3. Frequencies and Damping Values for Third Model

Event			1st Horizontal		2nd Horizontal	Vertical (a)	Vertical (b)
				ω_d			
07E	f	Hz	2.35	2.27	7.43	4.47	5.28
	m	%	68.2		31.8	100.0	100.0
	β_r	%	15.6		101.0	108.2	85.8
	β_s	%	10.8		10.7	0.1	0.1
	$\Sigma\beta$	%	26.4		99.0*	99.0*	85.9
07N	f	Hz	2.28	2.21	7.35	4.47	5.28
	m	%	68.3		31.7	100.0	100.0
	β_r	%	15.0		99.4	108.2	85.8
	β_s	%	9.8		9.5	0.1	0.1
	$\Sigma\beta$	%	24.8		99.0*	99.0*	85.9
16E	f	Hz	2.57	2.50	8.29	4.77	5.64
	m	%	68.2		31.8	100.0	100.0
	β_r	%	14.8		99.4	107.5	85.1
	β_s	%	8.4		8.4	0.1	0.1
	$\Sigma\beta$	%	23.2		99.0*	99.0*	85.2
16N	f	Hz	2.34	2.26	7.46	4.77	5.64
	m	%	68.2		31.8	100.0	100.0
	β_r	%	15.3		100.2	107.5	85.1
	β_s	%	9.9		9.7	0.1	0.1
	$\Sigma\beta$	%	25.2		99.0*	99.0*	85.2
06E	f	Hz	3.42	3.38	11.35	7.01	8.06
	m	%	67.9		32.1	100.0	100.0
	β_r	%	13.2		96.5	100.5	80.5
	β_s	%	2.6		2.5	0.1	0.1
	$\Sigma\beta$	%	15.8		99.0*	99.0*	80.6
06N	f	Hz	3.48	3.44	11.61	7.01	8.06
	m	%	67.9		32.1	100.0	100.0
	β_r	%	12.9		96.0	100.5	80.5
	β_s	%	2.3		2.3	0.1	0.1
	$\Sigma\beta$	%	15.2		98.3	99.0*	80.6

* Upper limit for response analysis by BSAP.

Note: For the Vertical, (a) and (b) refer to the models based on undamped and damped dimensionless frequencies.

The System Dimensionless Frequencies tabulated in Table 2 are for both the Undamped and Damped Systems. When system damping is small, it does not make a difference whether, in the calculation of the dimensionless frequency, the damped or undamped system frequency is used. However, when damping becomes large, as is the case for the vertical response, a distinct difference exists. The results reported herein are based on the damped dimensionless frequency.

Step 6. Input Motion

The common practice in SSM is to apply the free-field surface motion as the input to the soil-spring model. When embedment effects need to be considered, the character of the input motion changes drastically particularly for the horizontal-rocking mode (Hadjian and Tang, 1992). However, extensive evaluations (Hadjian, 1993) strongly suggest that little will be gained by modifying the input motion for vertical response analysis. The free-field surface ground motion can thus be used as the input motion for vertical excitation.

Step 7. System Response

At this step the final model with the appropriate total modal damping values (Step 5) and the input motions (Step 6) are combined to obtain the total response of the structure by the modal analysis method commonly available in structural analysis computer codes. Three sets of responses are calculated at two locations in the 1/4-scale containment: at about the top, station F4US, and at about the bottom, station F4LS. Refer to Fig. 1. To evaluate the results, the 5% damped response spectra of the time-history responses, both predicted and recorded, were calculated and plotted together for each location of response.

COMPARISON OF VERTICAL RESPONSE RESULTS

Although a comparison of predicted to recorded responses would be sufficient to determine the viability of the improved SSM, it would be useful to also compare the SSM results with those results obtained using more sophisticated procedures.

The synthesis report of the predictions and correlation studies of the Lotung SSI experiment (Hadjian et al, 1991) divided all the prediction and post-prediction solutions into two groups: The better solutions and the less successful solutions. Six solutions from the first group are selected to compare with the present SSM results. The selected solutions are listed below under "Other Methods/Models."

Event		Other Methods/Models	Prediction by
LSST07	Fig. 5	SASSI/B,C	Bechtel
LSST07	Fig. 6	CLASSI/A_{H1}	Luco/Wong
LSST07	Fig. 7	SUPERALUSH-CLASSI/D*	EQE/EET
LSST07	Fig. 8	SASSI/D*	Impell
LSST16	Fig. 9	SASSI/B,C	Bechtel
LSST16	Fig. 10	CLASSI (Bechtel)	Bechtel

*Post-Prediction Models

Since ratios of predicted to recorded response spectra are not available for the earlier solutions, and in order to achieve a fair comparison, the present SSM results are re-drawn to approximately match the same scales of the earlier figures. And finally, in order to better recognize overpredictions and underpredictions, the space between the predicted and recorded response spectra is shaded black when *underprediction* occurs.

The following is a summary evaluation of the above comparisons. Because of the relatively rigid model, there are no, for all practical purposes, differences in response between the top (F4US) and bottom (F4LS) of the containment. Only the top of containment results are presented.

Figure 5 - The SSM results are superior to the SASSI results.

Figure 6 - The SSM results are superior to the CLASSI results.

Figure 7 - The SSM results are superior to the SUPERALUSH/CLASSI results despite the latter being a Post-Prediction Model.

Figure 8 - The SSM results are superior to the SASSI results despite the latter being a Post-Prediction Model.

Figure 9 - The SSM and SASSI results are comparable.

Figure 10- The SSM results are slightly better, overall, than the CLASSI (Bechtel) results. The SSM under-prediction is larger between 2-4 Hz, but significantly better between 7-10 Hz. An evaluation of this underprediction is given below.

As shown in Fig. 11 a distinct mismatch of the peaks for Event LSST16 occurs between 2-3 Hz. Since F4US and F4LS are located along the containment wall, the rocking of the structure contributes significantly to the vertical response. Therefore, the differences in the response spectra are due to the horizontal rather than to the vertical response methodology. To validate this the horizontal and rocking spring values were increased by a factor of 1.44 and the response of the structure to both horizontal and vertical excitations recalculated. This change in soil-spring values modifies the undamped translational-rocking mode frequency in the NS direction from 2.34 Hz to 2.81 Hz and the mismatch of the peaks in Fig. 11 is eliminated as a consequence. These new results are shown in Fig. 12. Fig. 13 compares the ratios of the predicted to recorded response spectra for the original and modified soil-springs solutions. As seen in these figures a definite improvement in response comparisons has been achieved between about 1.4 - 4.0 Hz.

As expected, a similar improvement also occurs in the *horizontal* response comparisons. The response ratios for the NS response are compared in Fig. 14. Clearly, the match of calculated to recorded results throughout the frequency range has been improved. It can thus be concluded that the mismatch in Fig. 11 is due to inadequate modeling in the horizontal-rocking response mode. The above change in the spring values translates to a change in the earthquake degraded shear wave velocity of about 20%. The issue obviously is the determination of strain-dependent soil properties rather than the SSM analysis methodology.

CONCLUSIONS

The soil-spring method, as presented in this study, has proved to be a viable method to predict the vertical earthquake responses of the Lotung 1/4-scale containment to three earthquakes of different characteristics. The results obtained are beyond most optimistic expectations. Improvements, if any, are needed in the determination of the earthquake degraded soil parameters.

The comparisons of the SSM results, with results obtained using the state-of-the-art methods of SASSI and CLASSI, on the basis of similarly scaled figures, establishes the improved SSM for seismic SSI, as used herein, at least as a comparable analysis tool. Figures 5 through 10 clearly show that the SSM has produced, relative to the other methods, more successful overall predictions.

ACKNOWLEDGEMENT

Discussions with Prof. J. E. Luco throughout the development of the procedure discribed herein are gratefully acknowledged.

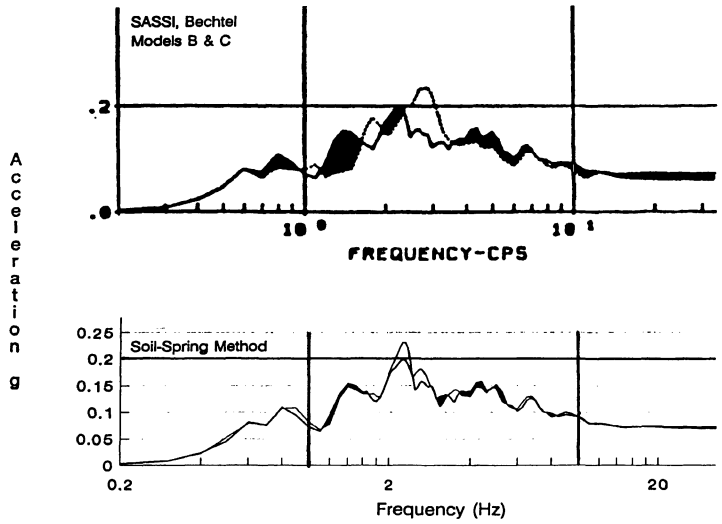

Fig. 5. Predicted and Recorded 5% Damped Response Spectra, Event LSST07, Vertical at F4US

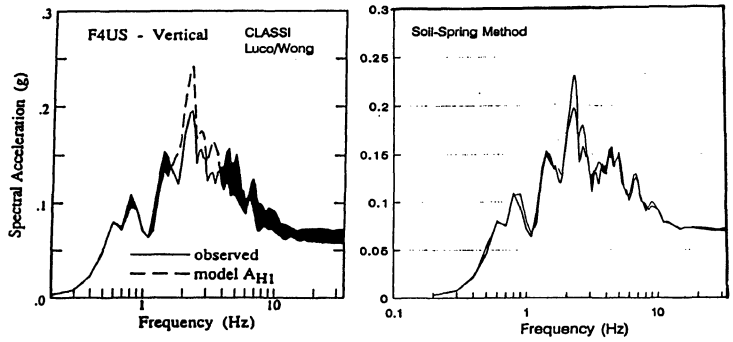

Fig. 6. Predicted and Recorded 5% Damped Response Spectra, Event LSST07, Vertical at F4US

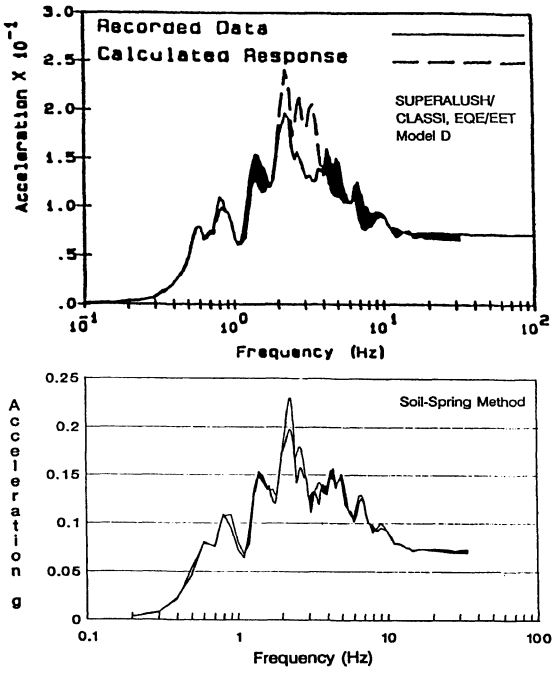

Fig. 7. Predicted and Recorded 5% Damped Response Spectra, Event LSST07, Vertical at F4US

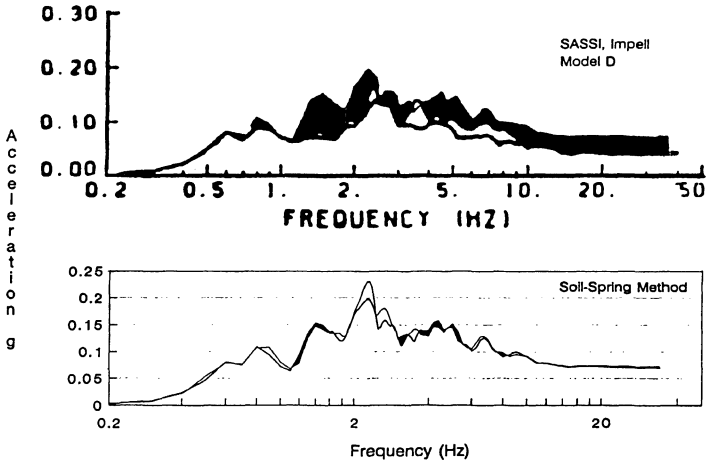

Fig. 8. Predicted and Recorded 5% Damped Response Spectra, Event LSST07, Vertical at F4US

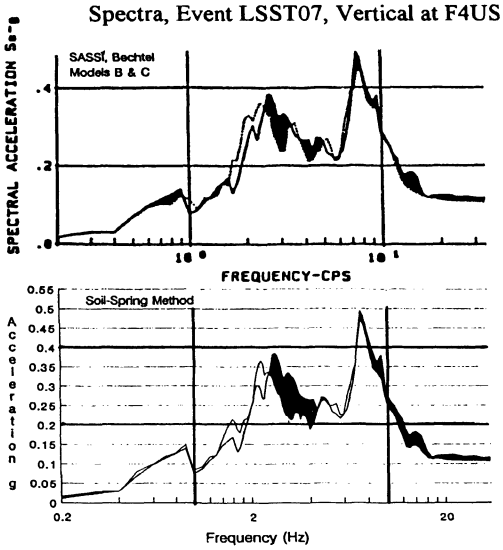

Fig. 9. Predicted and Recorded 5% Damped Response Spectra, Event LSST16, Vertical at F4US

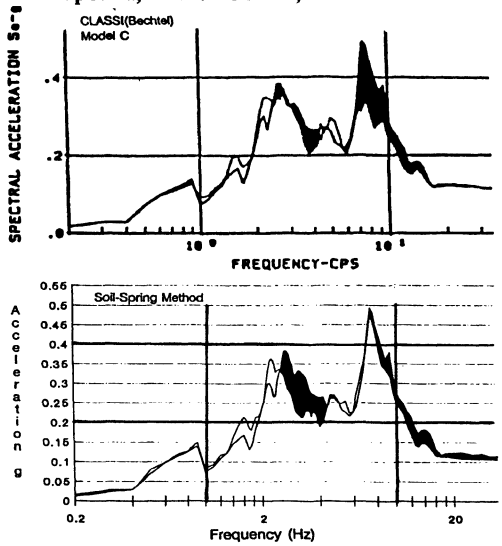

Fig. 10. Predicted and Recorded 5% Damped Response Spectra, Event LSST16, Vertical at F4US

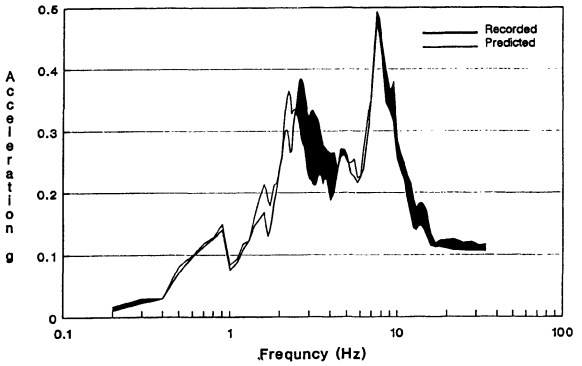

Fig.11. Recorded and Predicted 5% Damped Response Spectra, Event LSST16, Vertical at F4US

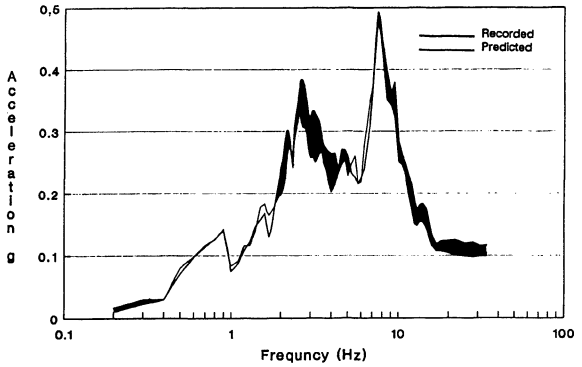

Fig.12. Recorded and Predicted 5% Damped Response Spectra, Event LSST16, Vertical, F4US, with Modified Soil-Springs

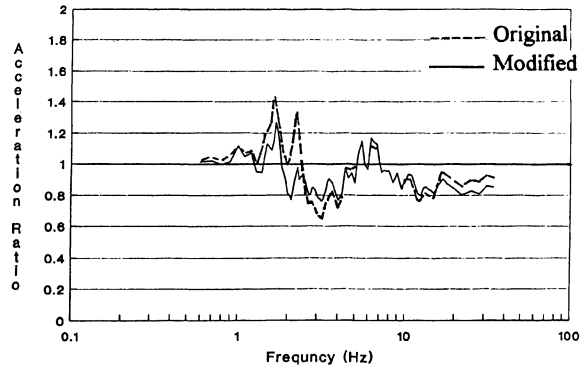

Fig. 13. Predicted to Recorded Spectra Ratios, Event LSST16, Vertical, F4US, with Original and Modified Soil-Springs

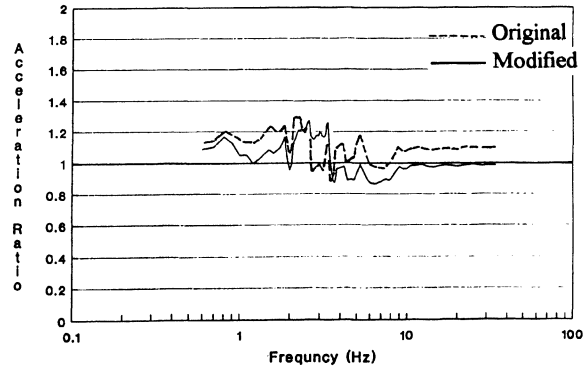

Fig. 14. Predicted to Recorded Spectra Ratios, Event LSST16, NS, F4US, with Original and Modified Soil Springs

REFERENCES

Anderson, D. G., (1991). *Geotechnical Synthesis Report for the Lotung Large-Scale Seismic Experiment,* Electric Power Research Institute, RP 2225-23 Final Report, October.

Aspel, R. J., (1979). *Dynamic Green's Function for Layered Media and Applications to Boundary Value Problems,* Ph.D. Thesis, University of California, San Diego.

Bechtel Corporation, (1992). *Seismic Analysis of Structures and Equipment for Nuclear Power Plants,* DG C-104.

Day, S.M., (1977). *Finite Element Analysis of Seismic Scattering Problems,* Ph.D. Dissertation, University of California, San Diego.

Gazetas, G., (1991). *Formulas and Charts for Impedances of Surface and Embedded Foundations,* ASCE, Journal of Geotechnical Engineering, Vol. 117, No. 9, Sept. pp. 1363-1381.

Geomatrix Consultants, (1991). *Analysis of Ground Response Data at Lotung Large Scale Seismic Test Site,* EPRI NP-7306, Palo Alto, California.

Hadjian, A. H., (1991). *The Soil-Spring Method for Seismic Soil-Structure Interaction Analysis - A Demonstration of Its Potential,* EPRI Draft Final Report, December.

Hadjian, A. H. (1993). *The Soil-Spring Method for Seismic Soil-Structure Interaction Analysis,* EPRI Draft Final Report, June.

Hadjian, A. H. and Ellison, B., (1985). *Equivalent Properties for Layered Media,* Soil Dynamics and Earthquake Engineering, Vol. 4, No. 4, pp. 203-209.

Hadjian, A. H., et al, (1991). *A Synthesis of Prediction Results and Correlation Studies of the Lotung Soil-Structure Interaction Experiment,* Electric Power Research Institute, EPRI NP-7307, Palo Alto, California, October.

Hadjian, A. H. and Tang, H. T., (1992). *Soil-Spring SSI Improvements Based on Test Correlations of the Lotung SSI Experiment - Horizontal Excitation, Proceedings,* Symposium on Current Issues Related to Nuclear Power Plant Structures, Equipment and Piping, Orlando, Florida, December.

Luco, J. E., (1976). *Vibration of a Rigid Disc on a Layered Visco-elastic Medium,* Nuclear Engineering and Design, Vol. 36, pp. 325-340.

Luco, J. E., (1980). *Soil-Structure Interaction and Identification of Structural Models,* Proceedings, ASCE Specialty Conference on Civil Engineering and Nuclear Power, Knoxville, Tennessee, September 15-17.

Luco, J. E. and Wong, H. L., (1979). *Response of Structures to Nonvertically Incident Seismic Waves,* Department of Applied Mechanics and Engineering, University of California, San Diego, La Jolla, California, October.

Luco, J. E., and Wong, H. L., (1989). *Prediction of the Forced Vibration and Seismic Response of the Lotung (Taiwan) Large-Scale Containment Model and Comparison with Observations,* Proc., EPRI/NRC/TPC Workshop, EPRI, NP-6154, Vol. 1, pp. 8-1 to 8-55.

Lysmer, J., Tabatabaie-Raissi, M., Tajirian, F., Vahdani, S., and Ostadan, F., (1981). *SASSI - A System for Analysis of Soil-Structures Interaction,* Report No. UCB/GT/8101, University of California, Berkely, April.

Mita, A., and Luco, J. E., (1989). *Impedence Functions and Input Motions for Embedded Square Foundations,* ASCE, Journal of Geotechnical Engineering, Vol. 115, No. 4, April, pp. 491-503.

Ohsaki Research Institute, Inc., (1989). *Geotechnical Test Report of Backfill for Lotung Project,* Draft Report Prepared for Tokyo Electric Company, Japan, June.

Prange, B., (1965). *Ein Beitrag zum Problem der Spannungsmessung in Halbraum,* Dissertation, Technischen Hochschule Karlsruhe, Germany, O. Berenz (Karlsruhe), 159 pp.

Richart, F. E., Hall, Jr., J. R., and Woods, R. D., (1970). *Vibration of Soils and Foundations,* Prentice-Hall, New Jersey.

Schnabel, P. B., Lysmer, J., and Seed, H. B., (1972). *SHAKE - A Computer Program for Earthquake Response Analysis of Horizontally Layered Sites,* Report No. EERC-71-12, University of California, Berkeley, December.

Tang, H. T., (1987). *Large-Scale Soil-Structure Interaction,* EPRI NP-5513-SR, Palo Alto, California, November.